INSTITUTE OF PHYSICS PUBLISHING WAVES IN RANDOM MEDIA

Waves Random Media **14** (2004) 499–511 PII: S0959-7174(04)78292-0

Multiple scattering effects on the radar cross section (RCS) of objects in a random medium including backscattering enhancement and shower curtain effects

Akira Ishimaru, Sermsak Jaruwatanadilok and Yasuo Kuga

Department of Electrical Engineering, Box 352500, University of Washington, Seattle, WA 98195, USA

E-mail: ishimaru@ee.washington.edu

Received 24 March 2004, in final form 18 May 2004
Published 14 June 2004
Online at stacks.iop.org/WRM/14/499
doi:10.1088/0959-7174/14/4/002

Abstract

This paper presents a theory of the radar cross section (RCS) of objects in multiple scattering random media. The general formulation includes the fourth-order moments including the correlation between the forward and the backward waves. The fourth moments are reduced to the second-order moments by using the circular complex Gaussian assumption. The stochastic Green's functions are expressed in parabolic approximation, and the objects are assumed to be large in terms of wavelength; therefore, Kirchhoff approximations are applicable. This theory includes the backscattering enhancement and the shower curtain effects, which are not normally considered in conventional theory. Numerical examples of a conducting object in a random medium characterized by the Gaussian and Henyey–Greenstein phase functions are shown to highlight the difference between the multiple scattering RCS and the conventional RCS in terms of optical depth, medium location and angular dependence. It shows the enhanced backscattering due to multiple scattering and the increased RCS if a random medium is closer to the transmitter.

1. Introduction

There has been extensive research on the radar cross section of rough surfaces and the atmosphere [1–4]. However, if an object is located within a random medium, its cross section is affected by multiple scattering in the medium. The wave incident upon the object consists of coherent and incoherent waves, and the scattered wave also experiences multiple scattering. In addition, the induced current on the object has coherent and incoherent components. To

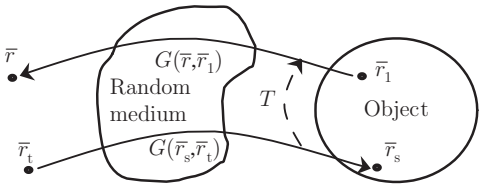

Figure 1. The Dirichlet object is illuminated by a transmitter at $\bar{r}_t$ through a random medium and the scattered wave is observed at $\bar{r}$.

obtain the stochastic induced current, we need to solve the stochastic surface integral equation for the object [5, 6]. In this paper, however, we assume that the object size and surface radius of curvature are much greater than the wavelength, and therefore, the Kirchhoff approximation is applicable to obtain the induced current. There are correlations between the incident and scattered waves in the medium. To take into account the above effects, we start with general formulations including stochastic Green's functions. We make use of the parabolic equation approximation for the stochastic Green's functions, which should be applicable to many practical problems in microwave and optical scattering in the atmosphere and the ocean, as well as optical scattering in biological media [4].

The formulation is based on the use of the circular complex Gaussian assumption. It includes two effects: backscattering enhancement [7, 8] and shower curtain effects [9]. Both phenomena have been discussed recently, but have not been included in most RCS studies. The backscattering enhancement effect is interesting as RCS can become higher than the conventional RCS, while the shower curtain effects give different RCS depending on whether the random medium is closer to or further from the transmitter.

2. Formulation of the problem

Let us consider a Dirichlet object in a random medium. The scattered field at $\bar{r}$ is given by [10]

$$\psi_s(\bar{r}) = -\int_s G(\bar{r}, \bar{r}_1)\frac{\partial \psi(\bar{r}_1)}{\partial n_1}\,\mathrm{d}S_1, \tag{1}$$

where G is the stochastic Green's function. In general, the random surface field $\partial\psi(\bar{r}_1)/\partial n_1$ can be expressed using the random transition (scattering) operator T,

$$\frac{\partial \psi(\bar{r}_1)}{\partial n_1} = \int T(\bar{r}_1, \bar{r}_s)\frac{\partial \psi_{in}(\bar{r}_s)}{\partial n_s}\,\mathrm{d}S, \tag{2}$$

where $\psi_{in}(\bar{r}_s)$ is the incident field at $\bar{r}_s$ as shown in figure 1.

Now, we assume that the object size and its surface radius of curvature are greater than the wavelength and the Kirchhoff approximation is applicable. Then, we get the well-known Kirchhoff surface field

$$\begin{aligned} &T(\bar{r}_1, \bar{r}_s) = 2\delta(\bar{r}_1 - \bar{r}_s), \\ &\frac{\partial \psi(\bar{r}_1)}{\partial n_1} = 2\frac{\partial \psi_{in}(\bar{r}_1)}{\partial n_1}. \end{aligned} \tag{3}$$

The scattered field is then given by

$$\psi_s(\bar{r}) = -2\int G(\bar{r}, \bar{r}_1)\frac{\partial \psi_i(\bar{r}_1)}{\partial n_1}\,\mathrm{d}S_1. \tag{4}$$

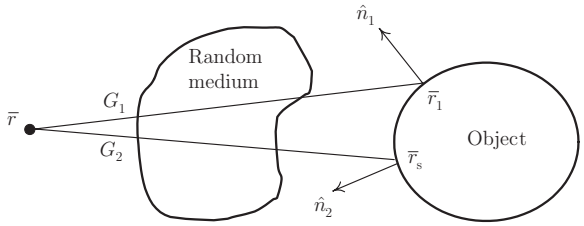

Figure 2. Stochastic Green's functions G_1 and G_2.

The scattered power at $\bar{r}$ is given by

$$\langle|\psi_s(\bar{r})|^2\rangle = 4\int\int \mathrm{d}S_1\,\mathrm{d}S_2\left\langle G_1\frac{\partial\psi_{i1}}{\partial n_1}G_2^*\frac{\partial\psi_{i2}^*}{\partial n_2}\right\rangle, \tag{5}$$

where $G_1 = G_1(\bar{r},\bar{r}_1)$, $\psi_{i1} = \psi_i(\bar{r}_1)$, $G_2 = G_2(\bar{r},\bar{r}_2)$, $\psi_{i2} = \psi_i(\bar{r}_2)$ as shown in figure 2.

This contains the fourth-order moment, and using the circular complex Gaussian assumption, we can express the fourth-order moment in terms of second-order moments [5]. (see the appendix)

$$\begin{aligned}\left\langle G_1\frac{\partial}{\partial n_1}\psi_{i1}G_2^*\frac{\partial}{\partial n_2}\psi_{i2}^*\right\rangle &= \langle G_1G_2^*\rangle\left\langle\frac{\partial}{\partial n_1}\psi_{i1}\frac{\partial}{\partial n_2}\psi_{i2}^*\right\rangle + \left\langle G_1\frac{\partial}{\partial n_2}\psi_{i2}^*\right\rangle\left\langle\frac{\partial}{\partial n_1}\psi_{i1}G_2^*\right\rangle\\ &\quad - \langle G_1\rangle\left\langle\frac{\partial}{\partial n_1}\psi_{i1}\right\rangle\langle G_2^*\rangle\left\langle\frac{\partial}{\partial n_2}\psi_{i2}^*\right\rangle.\end{aligned} \tag{6}$$

It is important to note that equation (6) includes the correlation between the incident ψ_i and the scattered field G, and this gives the backscattering enhancement to be discussed in a later section. In contrast, it is often assumed that there is no correlation between the incident and the scattered field and with this assumption, we get

$$\left\langle G_1\frac{\partial}{\partial n_1}\psi_{i1}G_2^*\frac{\partial}{\partial n_2}\psi_{i2}^*\right\rangle = \langle G_1G_2^*\rangle\left\langle\frac{\partial}{\partial n_1}\psi_{i1}\frac{\partial}{\partial n_2}\psi_{i2}^*\right\rangle. \tag{7}$$

We will show later the difference between our formulation in equation (6) and the formulation in equation (7).

The apparent RCS of the object is then given by

$$\mathrm{RCS} = \frac{4\pi L^2\langle|\psi_s|^2\rangle}{|\psi_o|^2}, \tag{8}$$

where ψ_o is the free space incident field at the object, ψ_s is the scattered field at the observation point and L is the distance between the object and the observation point.

We now examine equations (5) and (6). The incident wave ψ_i is the stochastic Green's function and we write

$$\begin{aligned}\psi_{i1} &= \psi(\bar{r}_1) = G_1(\bar{r},\bar{r}_1),\\ \psi_{i2} &= \psi(\bar{r}_2) = G_2(\bar{r},\bar{r}_2),\end{aligned} \tag{9}$$

where we used the reciprocity: $G_1(\bar{r},\bar{r}_1) = G_1(\bar{r}_1,\bar{r})$. Under the parabolic equation approximation [4, 10], Green's function is given by

$$G = (\text{slowly varying function of } z \text{ and } \bar{\rho})\exp(\mathrm{i}kz). \tag{10}$$

Therefore,

$$\frac{\partial}{\partial n} = -\mathrm{i}k\hat{s}\cdot\hat{n}_1 = -\mathrm{i}k(\hat{z}\cdot\hat{n}_1), \tag{11}$$

where $\hat{s} \approx \hat{z}$ is the direction of wave propagation. Using equations (9) and (11), we get

$$\langle|\psi_s|^2\rangle = 4k^2 \int\int (\mathrm{d}S_1\, \mathrm{d}S_2[\langle G_1\rangle^2\langle G_2^*\rangle^2 + 4\langle G_1\rangle\langle G_2^*\rangle\langle G_{f1}G_{f2}^*\rangle + 2\langle G_{f1}G_{f2}^*\rangle^2](\hat{z}\cdot\hat{n}_1)(\hat{z}\cdot\hat{n}_2)), \tag{12}$$

where $G = \langle G\rangle + G_f$, $\langle G\rangle$ is the coherent component and G_f is the incoherent component. Note that if we ignore the correlation between the incident and the scattered field as in equation (7), we have

$$\langle|\psi_s|^2\rangle = 4k^2 \int\int (\mathrm{d}S_1\, \mathrm{d}S_2[\langle G_1\rangle^2\langle G_2^*\rangle^2 + 2\langle G_1\rangle\langle G_2^*\rangle\langle G_{f1}G_{f2}^*\rangle + \langle G_{f1}G_{f2}^*\rangle^2](\hat{z}\cdot\hat{n}_1)(\hat{z}\cdot\hat{n}_2)). \tag{13}$$

The difference between equations (12) and (13) is that equation (12) includes the enhancement while equation (13) does not. We now need to evaluate equation (12) to obtain the RCS.

3. Stochastic Green's functions

Let us now evaluate equation (12). Under the parabolic approximation, we get

$$\begin{aligned}\langle G_1\rangle &= \frac{1}{4\pi L}\exp\left(\frac{\mathrm{i}k\rho_1^2}{2z_1} + \mathrm{i}kz_1 - \frac{\tau_\mathrm{o}}{2}\right),\\ \langle G_2\rangle &= \frac{1}{4\pi L}\exp\left(\frac{\mathrm{i}k\rho_2^2}{2z_2} + \mathrm{i}kz_2 - \frac{\tau_\mathrm{o}}{2}\right),\end{aligned} \tag{14}$$

where τ_o is the optical depth. We assume that the transmitter is in the far field of the object, and therefore $k\rho_1^2/z_1$ and $k\rho_2^2/z_2$ are negligibly small.

Next we consider the incoherent mutual coherence function

$$\langle G_{f1}G_{f2}^*\rangle = \Gamma_f(z_1, \bar{\rho}_1; z_2, \bar{\rho}_2). \tag{15}$$

The mutual coherence function Γ due to a point source has been obtained previously including the inhomogeneous random medium [4, 9, 11]

$$\begin{aligned}\Gamma = \Gamma(z_1, \bar{\rho}_1; z_2, \bar{\rho}_2) &= \langle G(z_1, \bar{\rho}_1)G^*(z_2, \bar{\rho}_2)\rangle\\ &= \frac{1}{(4\pi X)^2}\exp\left(-\mathrm{i}k\frac{\bar{\rho}_d\cdot\bar{\rho}_c}{X} - H + \mathrm{i}k(z_1 - z_2)\right),\end{aligned} \tag{16}$$

where $X = X(z) = \int_0^z \frac{\mathrm{d}z'}{n(z')}$, $H = \int_0^z a\,\mathrm{d}z' + \int_0^z b\,\mathrm{d}z'\frac{1}{2}\int_0^2 p(s)s\,\mathrm{d}s[1 - J_\mathrm{o}(kns\rho)]$. The phase function $p(s)$ is normalized so that

$$\frac{1}{2}\int_0^2 p(s)s\,\mathrm{d}s = 1, \tag{17}$$

$\rho = \left|\rho_d\frac{X(z')}{X(z)}\right|$, $n(z)$ is the refractive index, a is the absorption coefficient, b is the scattering coefficient and $s = 2\sin(\theta/2)$, θ = scattering angle. This is the mutual coherence function for a random medium consisting of a random distribution of particles.

First, we note that the term $k\bar{\rho}_d\cdot\bar{\rho}_c/X$ in the exponent is negligible when the transmitter is in the far field of the object. We then write the coherent Γ_c and incoherent Γ_i parts of Γ as

$$\begin{aligned}\Gamma &= \Gamma_\mathrm{c} + \Gamma_\mathrm{i},\\ \Gamma_\mathrm{c} &= \frac{1}{(4\pi X)^2}\exp(-\tau_\mathrm{o} + \mathrm{i}k(z_1 - z_2)),\\ \Gamma_\mathrm{i} &= \frac{1}{(4\pi X)^2}[\exp(-H) - \exp(-\tau_\mathrm{o})]\exp(\mathrm{i}k(z_1 - z_2)),\end{aligned} \tag{18}$$

where H is given in equation (16) and $H(\rho \to \infty) = \tau_o = \int_0^{d_2} (a+b)\,dz' =$ optical depth and d_2 is the thickness of the random medium.

Let us use the Henyey–Greenstein (HG) phase function for the scattering medium. We have

$$p(s) = \frac{(1-g)}{(1+g^2-2g\cos\theta)^{3/2}}, \qquad g = \text{anisotropy factor}, \tag{19}$$

which satisfies the normalization

$$\frac{1}{4\pi}\int_{4\pi} p(s)\,d\Omega = 1. \tag{20}$$

It is more convenient to use $s = 2\sin(\theta/2)$. Then, we write

$$\begin{aligned} p(s) &= \frac{(1+g)}{(1-g)^2}\frac{1}{\left[1+\left(\frac{s}{s_o}\right)^2\right]^{3/2}}, \qquad s_o = \frac{(1-g)^2}{g}, \\ &\frac{1}{2}\int_0^2 p(s)s\,ds = 1. \end{aligned} \tag{21}$$

Even though this is the HG phase function used for $0 < s < 2$ (or $0 < \theta < \pi$), it can be approximated by

$$\begin{aligned} p(s) &= \frac{2}{s_o}\frac{1}{\left[1+\left(\frac{s}{s_o}\right)^2\right]^{3/2}} \\ &\frac{1}{2}\int_0^\infty p(s)s\,ds = 1, \end{aligned} \tag{22}$$

when g is close to one. Making use of this, and using

$$\frac{1}{2}\int_0^\infty p(s)J_o(kns\rho)s\,ds = \exp(-kns_o\rho) \tag{23}$$

we get

$$H(\rho) = \int_0^z a\,dz' + \int_0^z b\,dz'[1-\exp(-kns_o\rho)]. \tag{24}$$

For large optical depth, the incoherent mutual coherence function Γ_i in equation (18) is well approximated by expanding $H(\rho)$ in equation (24) about $\rho = 0$ and keeping the first term

$$\Gamma_i = \frac{1}{(4\pi X)^2}\exp\left[-\int_0^z a\,dz' - \int_0^z b\,kns_o\rho\,dz'\right]. \tag{25}$$

A better approximation which reduces to the proper limit as the optical scattering depth $\tau_s \to 0$ and $\tau_s \to \infty$, and as $\rho \to 0$ and $\rho \to \infty$ is given by [11]

$$\Gamma_i = \frac{1}{(4\pi X)^2}\exp(-\tau_a)[1-\exp(-\tau_s)]\exp\left(-\frac{|\rho_d|}{|\rho_o|} + ik(z_1-z_2)\right), \tag{26}$$

where

$$\frac{1}{\rho_o} = \int_0^z b(z')kn(z')s_o\frac{X(z')}{X(z)}\,dz'[1-\exp(-\tau_s)]^{-1},$$

$\tau_a = \int_0^{d_2} a\,dz'$ is the optical absorption depth and $\tau_s = \int_0^{d_2} b\,dz'$ is the optical scattering depth. The coherence length ρ_o at the object is important to characterize RCS. If the uniform random medium with $n(z) = 1$ is located from d_1 to $d_1 + d_2$, we get

$$\frac{1}{\rho_o} = \frac{ks_o}{2}\frac{\left[(d_1+d_2)^2 - d_1^2\right]}{Ld_2}\tau_s[1-\exp(-\tau_s)]^{-1}. \tag{27}$$

If the phase function is given by the Gaussian function:

$$p(s) = 4\alpha_p \exp(-\alpha_p s^2) \tag{28}$$

with normalization $\frac{1}{2}\int_0^\infty p(s)s\,ds = 1$, the incoherent mutual coherence function Γ_i is given by

$$\Gamma_i = \frac{1}{X^2}\exp(-\tau_a)[1-\exp(-\tau_s)]\exp\left(-\frac{\rho_d^2}{\rho_o^2} + ik(z_1 - z_2)\right). \tag{29}$$

If the medium is uniform from d_1 to $d_1 + d_2$, we get

$$\frac{1}{\rho_o^2} = \frac{\tau_s k^2\left[(d_1+d_2)^3 - d_1^3\right]}{12\alpha_p L^2 d_2[1-\exp(-\tau_s)]}. \tag{30}$$

4. RCS of a large Dirichlet object

Making use of the stochastic Green's functions and the mutual coherence functions, we can now evaluate the apparent RCS given in equation (8). Noting equation (12), RCS is given by

$$\text{RCS} = \frac{4\pi L^2\langle|\psi_s|^2\rangle}{|\psi_o|^2} = I_1 + I_2 + I_3, \tag{31}$$

where I_1, I_2, I_3 are the three terms in equation (12). We note that in equation (12), we have

$$\int dS_1(\hat{z}\cdot\hat{n}_1) = \int d\hat{\rho}_1, \qquad \int dS_2(\hat{z}\cdot\hat{n}_2) = \int d\hat{\rho}_2. \tag{32}$$

Therefore, we have

$$\begin{aligned} I_1 &= \frac{4\pi}{\lambda^2}\exp(-2\tau_o)F_1, \\ I_2 &= \frac{4\pi}{\lambda^2}(4\exp(-\tau_o))[\exp(-\tau_a)(1-\exp(-\tau_s))]F_2, \\ I_3 &= \frac{4\pi}{\lambda^2}2[\exp(-\tau_a)(1-\exp(-\tau_s))]^2F_3, \end{aligned} \tag{33}$$

where

$$\begin{aligned} F_1 &= \int\int d\hat{\rho}_1\,d\hat{\rho}_2\exp(i2k(z_1-z_2)), \\ F_2 &= \int\int d\hat{\rho}_1 d\hat{\rho}_2\exp\left(i2k(z_1-z_2) - \frac{|\rho_d|}{|\rho_o|}\right) && \text{for HG medium,} \\ &= \int\int d\hat{\rho}_1\,d\hat{\rho}_2\exp\left(i2k(z_1-z_2) - \frac{\rho_d^2}{\rho_o^2}\right) && \text{for Gaussian medium,} \\ F_3 &= \int\int d\hat{\rho}_1\,d\hat{\rho}_2\exp\left(i2k(z_1-z_2) - \frac{2|\rho_d|}{|\rho_o|}\right) && \text{for HG medium,} \\ &= \int\int d\hat{\rho}_1\,d\hat{\rho}_2\exp\left(i2k(z_1-z_2) - \frac{2\rho_d^2}{\rho_o^2}\right) && \text{for Gaussian medium,} \end{aligned}$$

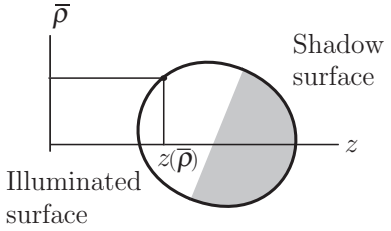

Figure 3. Illuminated surface given by $z = z(\bar{\rho})$.

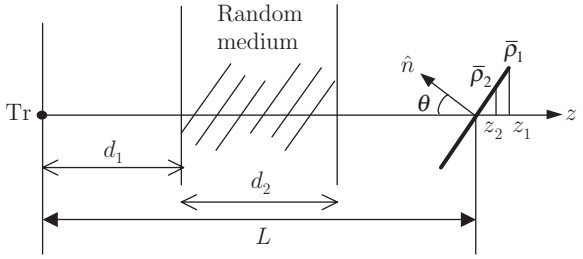

Figure 4. Inclined square conducting plate illuminated by the source. The random medium with thickness d_2 is located between the transmitter and the object. The plate size is $2a \times 2a$, and $\bar{\rho}_1 = x_1\hat{x} + y_1\hat{y}$ and $\bar{\rho}_2 = x_2\hat{x} + y_2\hat{y}$.

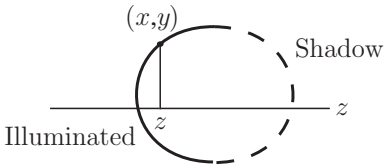

Figure 5. Spherical object.

and $\bar{\rho}_d = \bar{\rho}_1 - \bar{\rho}_2$, $\bar{\rho}_1 = x_1\hat{x} + y_1\hat{y}$, $\bar{\rho}_2 = x_2\hat{x} + y_2\hat{y}$. The illuminated surface of the object is given by $z = z_1(\hat{\rho}_1)$ and $z_2 = z_2(\hat{\rho}_2)$ as shown in figure 3. The coherence length ρ_o is given by equation (27) for a HG medium and by equation (30) for Gaussian medium.

For a large conducting plate shown in figure 4, we have $z(\rho) = x\tan\theta$,

$$\int\int \mathrm{d}\bar{\rho}_1\,\mathrm{d}\bar{\rho}_2 = \int_{-a\cos\theta}^{a\cos\theta}\mathrm{d}x_1\int_{-a}^{a}\mathrm{d}y_1\int_{-a\cos\theta}^{a\cos\theta}\mathrm{d}x_2\int_{-a}^{a}\mathrm{d}y_2, \tag{34}$$

and $z_1 - z_2 = (x_1 - x_2)\tan\theta$, $\rho_d = \sqrt{(x_1 - x_2)^2 + (y_1 - y_2)^2}$. The integral in (34) can be calculated numerically.

For a sphere with radius a shown in figure 5, we use

$$\int\int \mathrm{d}\bar{\rho}_1\,\mathrm{d}\bar{\rho}_2 = \int_0^a \rho_1\,\mathrm{d}\rho_1\int_0^{2\pi}\mathrm{d}\phi_1\int_0^a \rho_2\,\mathrm{d}\rho_2\int_0^{2\pi}\mathrm{d}\phi_2, \tag{35}$$

and $z_1 = a - \sqrt{a^2 - x_1^2 - y_1^2}$, $z_2 = a - \sqrt{a^2 - x_2^2 - y_2^2}$, $|\bar{\rho}| = \sqrt{(x_1 - x_2)^2 + (y_1 - y_2)^2}$, $x_1 = \rho_1\cos\phi_1$, $y_1 = \rho_1\sin\phi_1$, $x_2 = \rho_2\cos\phi_2$, $y_2 = \rho_2\sin\phi_2$.

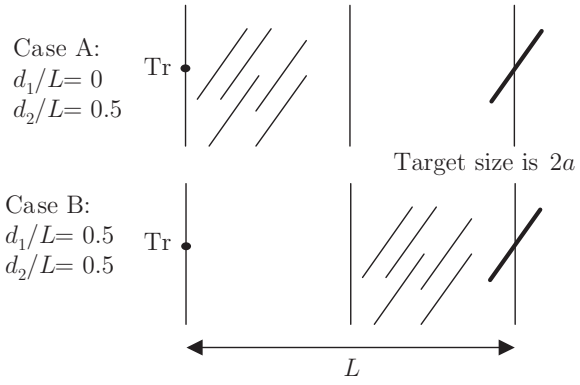

Figure 6. Geometry of RCS calculations.

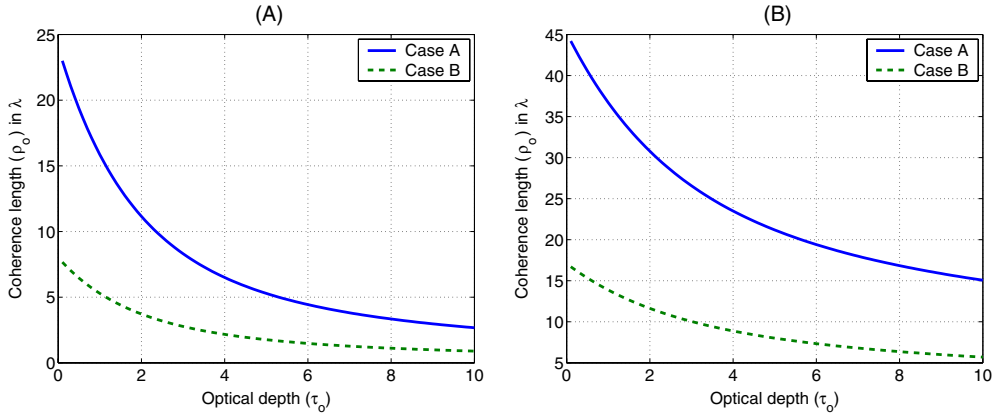

Figure 7. Coherence length for (A) Henyey–Greenstein phase function with albedo $(W_o) = 0.9$ and $g = 0.85$ and (B) Gaussian phase function with $W_o = 0.9$ and α_p which gives the same half-power beamwidth.

5. Coherence length and shower curtain effects

Equations (27) and (30) give general expressions of coherence length ρ_o for HG and Gaussian media. It is seen that ρ_o in terms of the wavelength depends on the optical scattering depth τ_s, the medium characteristics (s_o and α_p) and the ratio of the distances (d_1/L and d_2/L). In figures 6 and 7, we show the geometry and the coherence length in wavelength for case A and case B. Note that if the medium is close to the transmitter (case A), the coherence length is greater than case B, showing the shower curtain effect. For a HG medium, we use $W_o = 0.9$ and $g = 0.85$ where W_o is the albedo defined by $W_o = \frac{b}{a+b}$. For a Gaussian medium, we use $W_o = 0.9$ and α_p which gives the same half-power beamwidth as HG with $g = 0.85$.

6. RCS of a square plate

Let us examine the RCS of the square plate shown in figure 4. The plate size $2a$ is 3λ. In figure 8, we show I_1, I_2, I_3 and $I_{com} = I_1+I_2+I_3$ at $\theta = 0$. Note that I_1 is the conventional RCS

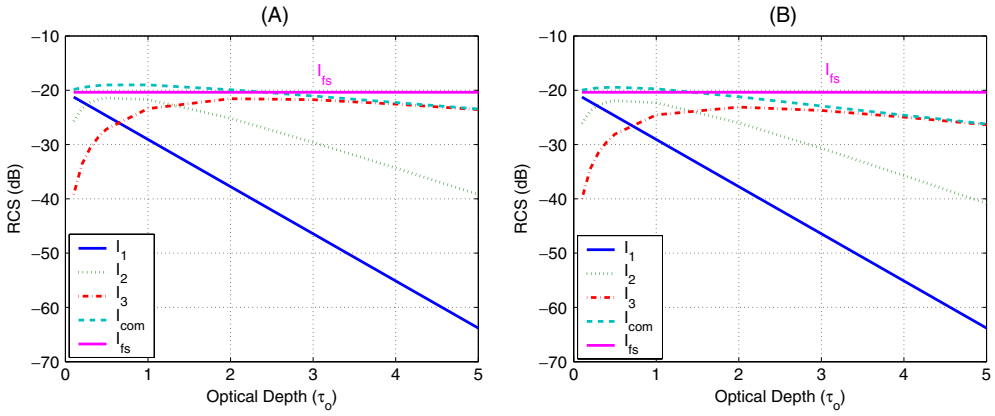

Figure 8. Components of RCS. Phase function is Henyey–Greenstein with albedo $(W_o) = 0.9$ and $g = 0.85$ in all case. (A) Case A geometry, (B) case B geometry. fs denotes free space. I_{fs} denotes the free space RCS.

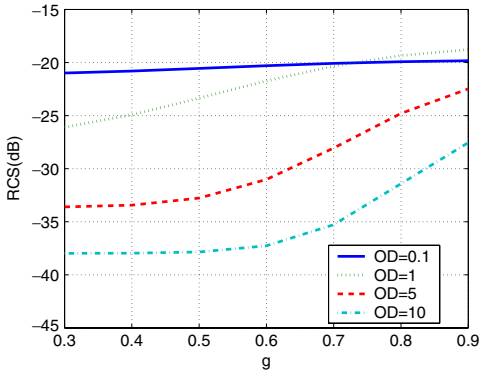

Figure 9. Effect of asymmetry factor g.

in a scattering medium and I_{com} is increasingly larger than I_1 as the optical depth increases. This indicates that the multiple scattering contributes significantly to the total RCS. The effects of asymmetry factor g and the albedo W_o are shown in figures 9 and 10, respectively. It shows that as g increases, the scattering pattern becomes more peaked in the forward direction and as W_o increases, the scattering increases, resulting in increased RCS.

We also compare the RCS from the geometry of case A and case B, which are shown in figure 11. Note that if the medium is close to the transmitter (case A), the RCS is higher than that of case B where the random medium is away from the transmitter. This result illustrates the shower curtain effect. Figure 12 shows the shower curtain effects as the random medium moves from $d_1 = 0$ to $d_1 = L/2$.

Figure 13 compares RCS, which includes backscattering enhancement from equation (12) with RCS without enhancement from equation (13). Note that the enhancement approaches 3 dB for large optical depth. Figure 14 shows the angular dependence of RCS at an optical depth of 1 and 5. It is shown that RCS, as a function of angle, is very much affected by

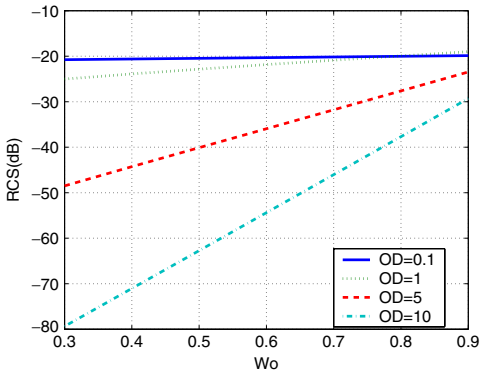

Figure 10. Effect of albedo W_o.

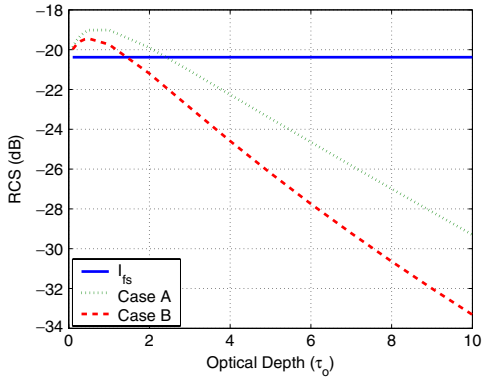

Figure 11. The shower curtain effect with Henyey–Greenstein phase function for geometry in case A and case B geometry. I_{fs} denotes the free space RCS.

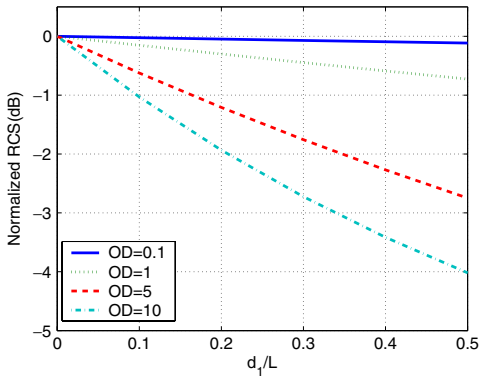

Figure 12. The shower curtain effect as a function of d_1/L.

the multiple scattering. This is more pronounced for large optical depth where RCS is quite different from the conventional RCS (I_1).

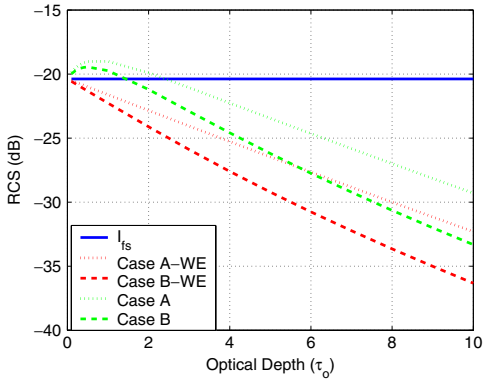

Figure 13. RCS comparison for the cases with and without backscattering enhancement. WE denotes without enhancement. I_{fs} denotes the free space RCS.

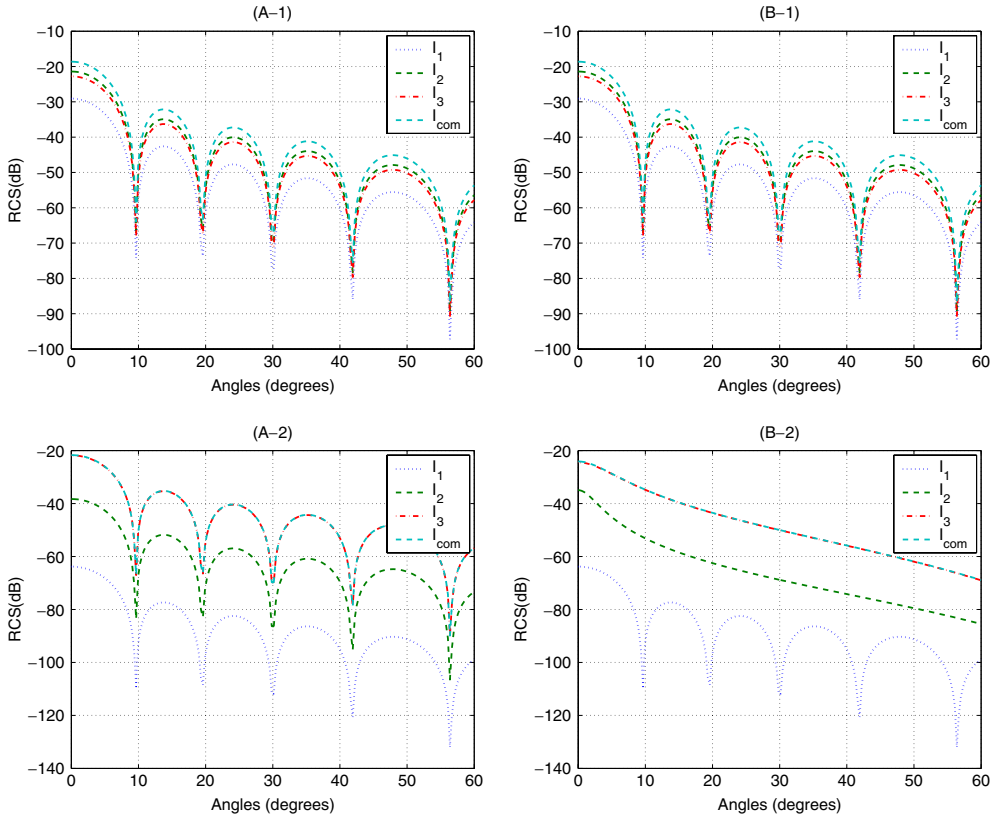

Figure 14. Angular dependence of RCS with Henyey–Greenstein phase function. (A-1) Case A with an optical depth (OD) of 1, (A-2) case A with an optical depth (OD) of 5, (B-1) case B with an optical depth (OD) of 1, and (B-2) case B with an optical depth (OD) of 5.

7. Conclusions

A theory of RCS in a multiple scattering environment is given by equations (8) and (12). This is applied to a flat conducting plate. The conventional RCS is given by I_1 and the multiple scattering RCS is given by $I_1 + I_2 + I_3$ in equation (33). The shower curtain effect, the backscattering enhancement and the angular dependence are shown to highlight the difference between the conventional RCS and the multiple scattering RCS.

Acknowledgments

This work is supported by the National Science Foundation (grant ECS-9908849) and the Office of Naval Research (grant N00014-04-1-0074).

Appendix. Circular complex Gaussian random variable [12, 13, 5]

Consider a complex random function u and its fluctuation v

$$u = \langle u \rangle + v. \tag{A.1}$$

Two circular complex Gaussian random variables u_1 and u_2 satisfy the following conditions:

$$\langle v_1 v_2 \rangle = 0, \qquad \text{but} \quad \langle v_1 v_2^* \rangle \neq 0 \tag{A.2}$$

and the odd moments of v are zero. Thus, the following relations hold

$$\langle v_1 v_2 v_3^* v_4^* \rangle = \langle v_1 v_3^* \rangle \langle v_2 v_4^* \rangle + \langle v_1 v_4^* \rangle \langle v_2 v_3^* \rangle$$

$$\begin{aligned}\langle u_1 u_2 u_3^* u_4^* \rangle &= \langle u_1 u_3^* \rangle \langle u_2 u_4^* \rangle + \langle u_1 u_4^* \rangle \langle u_2 u_3^* \rangle - \langle u_1 \rangle \langle u_2 \rangle \langle u_3^* \rangle \langle u_4^* \rangle \\ &= \langle u_1 \rangle \langle u_3^* \rangle \langle u_2 \rangle \langle u_4^* \rangle + \langle u_1 \rangle \langle u_3^* \rangle \langle v_2 v_4^* \rangle + \langle u_2 \rangle \langle u_4^* \rangle \langle v_1 v_3^* \rangle \\ &\quad + \langle v_1 v_3^* \rangle \langle v_2 v_4^* \rangle + \langle u_1 \rangle \langle u_4^* \rangle \langle v_2 v_3^* \rangle + \langle u_2 \rangle \langle u_3^* \rangle \langle v_1 v_4^* \rangle + \langle v_1 v_4^* \rangle \langle v_2 v_3^* \rangle\end{aligned}$$

$$\begin{aligned}\left\langle u_1^2 u_2^{*2} \right\rangle &= 2\langle u_1 u_2^* \rangle^2 - \langle u_1 \rangle^2 \langle u_2^* \rangle^2 \\ &= \langle u_1 \rangle^2 \langle u_2^* \rangle^2 + 4\langle u_1 \rangle \langle u_2^* \rangle \langle v_1 v_2^* \rangle + 2\langle v_1 v_2^* \rangle^2\end{aligned}$$

$$\langle u_1 u_2 \rangle = \langle u_1 \rangle \langle u_2 \rangle + \langle v_1 v_2 \rangle = \langle u_1 \rangle \langle u_2 \rangle.$$

We have applied this assumption to the wave propagation in a random medium. We found that the results reduce to the correct limits in the weak fluctuation as well as the strong fluctuation, and that the phenomena such as the backscattering enhancement result from the use of this assumption. Note that the circular complex Gaussian variables are similar to but different from the real Gaussian random variables [13].

References

[1] Kim H and Johnson J T 2002 Radar images of rough surface scattering: comparison of numerical and analytical models *IEEE Trans. Antennas Propag.* **50** 94–100

[2] Hesany V, Plant W J and Keller W C 2000 The normalized radar cross section of the sea at 10° incidence *IEEE Trans. Geosci. Remote. Sens.* **38** 64–72

[3] Bissonnette L R, Roy G, Poutier L, Cober S G and Isaac G A 2002 Multiple-scattering lidar retrieval method: tests on Monte Carlo simulations and comparisons with *in situ* measurements *Appl. Opt.* **41** 6307–24

[4] Ishimaru A 1997 *Wave Propagation and Scattering in Random Media* (New York: IEEE)

[5] Rockway J D 2001 Integral equation formulation for object scattering above a rough surface *PhD Dissertation* Dept. of Electrical Engineering, University of Washington, Seattle, WA

[6] Ocla H E and Tateiba M 2002 The effect of H-polarization on backscattering enhancement for partially convex targets of large sizes in continuous random media *Waves Random Media* **13** 125–36

[7] Ishimaru A 1991 Backscattering enhancement: from radar cross sections to electron and light localizations to rough surface scattering *IEEE Antennas Propag. Mag.* **33** 7–11
[8] Kuga Y and Ishimaru A 1984 Retroreflectance from a dense distribution of spherical particles A **1** 831–5
[9] Kuga Y and Ishimaru A 1986 Modulation transfer function of layered inhomogeneous random media using the small-angle approximation *Appl. Opt.* **25** 4382–5
[10] Ishimaru A 1991 *Electromagnetic Wave Propagation, Radiation, and Scattering* (Englewood Cliffs, NJ: Prentice Hall)
[11] Ishimaru A 1978 Limitation on image resolution imposed by a random medium *Appl. Opt.* **17** 348–52
[12] Goodman J W 1985 *Statistical Optics* (New York: Wiley)
[13] Middleton D 1960 *Introduction to Statistical Communication Theory* (New York: McGraw-Hill)